Self-Assembly of Medium-Chain Alkyl Monoglucosides in Ammonium Sulfate Solutions with Poly(ethylene glycol)

M. Gabriella Santonicola, Mark A. Yocum, II, Abraham M. Lenhoff, and Eric W. Kaler*

Center for Molecular and Engineering Thermodynamics, Department of Chemical Engineering, University of Delaware, Newark, Delaware 19716

Received November 24, 2006. In Final Form: February 10, 2007

We study the phase behavior and microstructure of alkyl-β-monoglucosides with intermediate chain lengths (octyl- and nonyl-β-glucoside) in aqueous solutions containing ammonium sulfate and poly(ethylene glycol) (PEG). When the glucoside surfactants are mixed with PEG of molecular weight 3350 or larger, two different phase transitions are observed in the temperature range 0−100 °C, with lower and upper miscibility gaps separated by a one-phase isotropic region. Isothermal titration calorimetry is used to quantify the effect of PEG on the micellization properties of the alkyl monoglucosides, whereas small-angle neutron scattering gives insight into the microstructure of the surfactant/polymer mixtures near the liquid−liquid phase boundary. Results show that the range and the strength of the interactions in these solutions are highly affected by the presence of PEG. Solutions with nonyl-β-glucoside contain larger micelles than those with octyl-β-glucoside, and the intermicellar interactions are much stronger and longer ranged. The relevance of these findings for membrane protein crystallization is discussed.

Introduction

Alkyl monoglucosides, especially medium-chain ones like octyl-β-glucoside ($C_8\beta G_1$) and nonyl-β-glucoside ($C_9\beta G_1$) that do not present Krafft boundaries, have achieved wide use in membrane protein applications, because of their nontoxic nature and their ability to solubilize these proteins outside biological membranes with minimal impact on their native conformation. Despite these properties, $C_8\beta G_1$ and $C_9\beta G_1$ are not optimal environments for crystallizing membrane proteins because they are completely miscible in water from 0 to 100 °C and for concentrations up to 60 wt %.[1] Many crystallization conditions, in fact, have been reported to be near liquid−liquid phase transitions,[2] and these are generally induced by adding precipitating agents such as polymers, salts, or other surfactants.[3]

Poly(ethylene glycol) (PEG) is the most common additive used to promote crystallization of both soluble and membrane proteins. In solutions of membrane proteins and alkyl polyglucosides, the effectiveness of PEG as a crystallizing agent has been linked to a liquid−liquid phase separation that develops around room temperature, and qualitative phase diagrams showing this phenomenon are available in the literature.[2,4] However, the mechanism of phase separation in these mixtures and the nature of the interactions near the liquid−liquid phase separation, which are relevant to the induction of crystallization, remain open questions.

Although mixtures of oppositely charged polymers and surfactants are studied extensively, there is much less information available about how uncharged polymers interact with nonionic surfactants. The phase behavior of ethoxylated surfactants in solutions with PEG has been studied by Wormuth[5] and Piculell et al.[6] In both studies, a segregative phase separation was observed that is similar to the separation in mixtures of two nonionic polymers, such as PEG and dextran.[7,8] Unlike medium-chain alkyl monoglucosides, solutions of ethoxylated surfactants display liquid−liquid phase separations with increasing temperature even in the absence of polymers. Addition of PEG lowers the upper miscibility gap and also induces a separate miscibility region at lower temperatures. The upper and lower two-phase regions eventually merge as the amphiphilicity of the surfactant or the polymer molecular weight is increased.[5] Piculell et al. also report that in mixtures of $C_8\beta G_1$ and PEO 40 000 the high molecular weight polymer induces a phase separation at low temperature with typical segregative features.[6]

Intermicellar interactions are known to play a fundamental role in setting the overall interactions among the complexes that form between membrane proteins and surfactants.[4] It is likely that, when these attractions are appropriately attractive, membrane protein crystallization can occur. Techniques such as static light scattering and self-interaction chromatography are used to characterize protein−protein interactions in terms of the osmotic second virial coefficient (B_{22}).[9,10] In the case of soluble proteins, protein crystallization conditions were found to correlate with a range of small negative values of B_{22}, an observation defining the concept of a "crystallization slot".[11] Extending this concept to solutions of membrane proteins and surfactants is more challenging due to the presence of both protein−surfactant complexes and micellar aggregates in solution. However, several

* To whom correspondence should be addressed. E-mail: kaler@udel.edu. Phone: (302)831-3553. Fax: (302)831-6751.

(1) Nilsson, F.; Söderman, O.; Hansson, P.; Johansson, I. *Langmuir* **1998**, *14*, 4050−4058.
(2) Garavito, R. M.; Markovic-Housley, Z.; Jenkins, J. A. *J. Cryst. Growth* **1986**, *76*, 701−709.
(3) Michel, H. *Crystallization of Membrane Proteins*; CRC Press: Boca Raton, FL, 1991.
(4) Zulauf, M. In *Crystallization of Membrane Proteins*; Michel, H., Ed.; CRC Press: Boca Raton, FL, 1991.
(5) Wormuth, K. R. *Langmuir* **1991**, *7*, 1622−1626.
(6) Piculell, L.; Bergfeldt, K.; Gerdes, S. *J. Phys. Chem.* **1996**, *100*, 3675−3679.
(7) Zaslavsky, B. Y.; Bagirov, T. O.; Borovskaya, A. A.; Gulaeva, N. D.; Miheeva, L. H.; Mahmudov, A. U.; Rodnikova, M. N. *Polymer* **1989**, *30*, 2104−2111.
(8) Saeki, S.; Kuwahara, N.; Hamano, K.; Kenmochi, Y.; Yamaguchi, T. *Macromolecules* **1986**, *19*, 2353−2356.
(9) George, A.; Chiang, Y.; Guo, B.; Arabshahi, A.; Cai, Z.; Wilson, W. W. *Macromol. Crystallogr., Part A* **1997**, *276*, 100−110.
(10) Tessier, P. M.; Lenhoff, A. M.; Sandler, S. I. *Biophys. J.* **2002**, *82*, 1620−1631.
(11) George, A.; Wilson, W. W. *Acta Crystallogr. Sect. D* **1994**, *50*, 361−365.

10.1021/la063427d CCC: $37.00
Published on Web 04/13/2007

authors have tried to assess the role of surfactant interactions in setting the overall interaction between complexes.[12,13]

Here, we report on the effects of PEG on the phase behavior and microstructure of octyl-β-glucoside ($C_8\beta G_1$) and nonyl-β-glucoside ($C_9\beta G_1$) in solutions with ammonium sulfate, which are commonly used in membrane protein crystallization. Using isothermal titration calorimetry (ITC) we study how the micellization process of the alkyl monoglucosides is affected by the polymer, while small-angle neutron scattering (SANS) is used to characterize the strength and range of the interactions for solution conditions near the liquid−liquid phase transition. The goal is to understand the effect of the polymer on the microstructure of these surfactant solutions so as to guide rationally the choice of membrane protein crystallization conditions. In addition, these studies are useful in optimizing protocols for extraction and purification of both hydrophilic and hydrophobic proteins by phase separation[14] and contribute to understanding the mechanism of PEG-induced partitioning in lipid membranes.[15]

Experimental Section

Materials. PEGs with molecular weights of 400, 1000, 3350, 8000, and 10 000 g·mol^{-1} were purchased from Sigma-Aldrich and were of Sigma Ultra grade. Alkyl monoglucosides $C_8\beta G_1$ and $C_9\beta G_1$ were purchased from Anatrace Inc. (Anagrade, purity >99%). Ammonium sulfate and potassium phosphate salts were from Sigma-Aldrich (BioChemika Ultra, ≥99.5%). Deuterium oxide (DLM-11, 99.9% deuterated, low paramagnetic) was obtained from Cambridge Isotope Laboratories and used as received.

Sample Preparation. Samples for phase behavior were prepared on a weight basis by dissolving surfactant and polymer in buffered salt solutions. Salt solutions were prepared with deionized water and filtered with a 0.2 μm syringe filter (Whatman, Anotop) before preparation of the PEG/glucoside samples. All salt solutions were buffered to avoid pH changes due to the slightly acidic nature of the glucosides. A pH of 5.5 (with 25 mM K_2HPO_4/KH_2PO_4) was chosen to parallel work on the membrane protein bacteriorhodopsin, which has been reported to be most stable for values of pH values between 5 and 6.[16]

Phase Behavior. The phase behavior of ternary mixtures of glucosides, PEG, and buffer solution was studied at constant pressure varying three independent variables: the temperature T, the total concentration by weight of PEG and surfactant in solution, γ, defined as

$$\gamma = \frac{\text{wt PEG} + \text{wt } C_i\beta G_1}{\text{wt PEG} + \text{wt } C_i\beta G_1 + \text{wt buffer}} \times 100\% \qquad (1)$$

and the mass ratio of PEG to the total amount of PEG and surfactant in the mixture, δ, defined as

$$\delta = \frac{\text{wt PEG}}{\text{wt PEG} + \text{wt } C_i\beta G_1} \times 100\% \qquad (2)$$

Phase behavior investigations were performed on mixtures with fixed δ and values of γ in the range of 0−25 wt %. Samples were placed in a constant temperature water bath, and the number of phases was examined at each temperature in the range of 0−100 °C. Equilibration times varied between a few hours and one week depending on the phases and concentrations. Phase boundaries were determined with an accuracy of ±0.1 °C. The ternary phase diagrams were mapped at 25 °C.

Colorimetric Determination of Alkyl Polyglucoside Surfactants. The concentration of alkyl polyglucosides in aqueous solutions was quantified using the anthrone method, a colorimetric assay developed for carbohydrates[17] and adapted to surfactants with glucose head groups.[18] The procedure is based on the formation of a complex between anthrone and the hydrolyzed glucose head group of the surfactant. The anthrone−glucose complex is green and has a maximum in absorption around 620 nm. Briefly, solutions of alkyl polyglucosides are boiled with the anthrone reagent (80 mg of anthrone/100 mL of concentrated sulfuric acid) until the green complex forms. The concentration of the glucoside is quantified by measuring the solution absorbance at 620 nm and comparing with a calibration curve. The standard deviation of the sample absorbance on the average of three measurements is 3% at most. Before the assay, concentrated samples of alkyl glucosides were diluted with deionized water to ensure that the APG concentration was in the range of applicability of the method. There was no effect of PEG on the outcome of the anthrone test, which was assessed by measuring samples with and without polymer at a known glucoside concentration.

Isothermal Titration Calorimetry. Experiments were performed using a VP-ITC microcalorimeter (MicroCal LLC, Northampton, MA). Detailed descriptions of the instrument and its application to measuring surfactant micellization are in the literature.[19−24] In each experiment 40 aliquots (6 μL each) of a stock solution of alkyl polyglucoside (10−15 times more concentrated than the estimated CMC) were automatically injected into a sample cell initially filled with pure solvent. The companion reference cell was filled with deionized water. The injections were added at 600-s intervals to allow the solution enough time to reach equilibrium after each injection (the cell was continuously stirred at 300 rpm). The enthalpy of mixing of surfactant and polymer was determined by integrating the raw heats recorded by the instrument at each injection and subtracting the heat evolved from dilution of the pure buffer. The CMC value was determined at the point where the first derivative curve of the ITC thermogram displays an extremum. The error of this evaluation is in the range of 1−2%.

Light Scattering. Dynamic light scattering experiments were performed with a Brookhaven apparatus equipped with a BI-200SM goniometer and a BI-9000AT correlator. The light source was a Lexel 95-3 argon-ion laser used at a wavelength of 488 nm and a maximum output power of 1000 mW. Samples were held in a temperature-controlled chamber with stability ±0.01 °C. Measurements were performed at a scattering angle of 90°, and the autocorrelation functions were analyzed using CONTIN,[25,26] provided with the correlator. The viscosities of the solvents were measured using a capillary viscometer where appropriate.

Small-Angle Neutron Scattering. Small-angle neutron scattering experiments were performed at the Center for High Resolution Neutron Scattering of the National Institute of Standards and Technology (NIST) in Gaithersburg, MD. In SANS experiments, the orientation-averaged intensities of neutrons scattered by particles in solution are measured as a function of the length of the scattering vector, $q = 4\pi/\lambda \sin(\theta/2)$, where θ is the angle between the scattered

(12) Hitscherich, C.; Kaplan, J.; Allaman, M.; Wiencek, J.; Loll, P. J. *Protein Sci.* **2000**, *9*, 1559−1566.
(13) Loll, P. J.; Allaman, M.; Wiencek, J. *J. Cryst. Growth* **2001**, *232*, 432−438.
(14) Saitoh, T.; Tani, H.; Kamidate, T.; Kamataki, T.; Watanabe, H. *Anal. Sci.* **1994**, *10*, 299−303.
(15) Lehtonen, J. Y. A.; Kinnunen, P. K. J. *Biophys. J.* **1995**, *68*, 525−535.
(16) Ludmann, K.; Gergely, C.; Varo, G. *Biophys. J.* **1998**, *75*, 3110−3119.
(17) Trevelyan, W. E.; Forrest, R. S.; Harrison, J. S. *Nature* **1952**, *170*, 626−627.
(18) Buschmann, N.; Wodarczak, S. *Tenside Surfactants Deterg.* **1995**, *32*, 336−339.
(19) Blandamer, M. J.; Cullis, P. M.; Engberts, J. *J. Chem. Soc. Faraday Trans.* **1998**, *94*, 2261−2267.
(20) Ohta, A.; Murakami, R.; Takiue, T.; Ikeda, N.; Aratono, M. *J. Phys. Chem. B* **2000**, *104*, 8592−8597.
(21) Ohta, A.; Miyagishi, S.; Aratono, M. *J. Phys. Chem. B* **2001**, *105*, 2826−2832.
(22) Blandamer, M. J.; Briggs, B.; Cullis, P. M.; Engberts, J. *Phys. Chem. Chem. Phys.* **2000**, *2*, 5146−5153.
(23) Blandamer, M. J.; Briggs, B.; Cullis, P. M.; Engberts, J.; Kevelam, J. *Phys. Chem. Chem. Phys.* **2000**, *2*, 4369−4372.
(24) Dai, S.; Tam, K. C. *Colloids Surf. A* **2003**, *229*, 157−168.
(25) Provencher, S. W. *Comput. Phys. Commun.* **1982**, *27*, 213−227.
(26) Provencher, S. W. *Comput. Phys. Commun.* **1982**, *27*, 229−242.

and incident beams. Here, the average neutron wavelength was 6 Å with a spread $\Delta\lambda/\lambda$ of 15%. Data were collected on the NG-3 instrument at sample detector distances of 1.33, 4.5, and 13 m, covering a q-range of 0.004−0.5 Å^{-1} (with a detector offset of 25 cm from the center at the shortest distance). Samples were held in quartz cells of 2 mm optical path length and left to equilibrate at the temperature of interest before being transferred to the temperature-controlled sample chamber. The acidity of buffer solutions in D_2O was measured with a glass electrode and corrected by adding 0.4 units to take into account the difference in pH meter reading between H_2O and D_2O solutions ($pD = pH_{reading} + 0.4$).[27] The raw scattering data were corrected for solvent, empty cell, and buffer solution scattering, all measured separately and placed on an absolute scale using standards calibrated by NIST. Scattering data were analyzed with the generalized indirect Fourier transformation (GIFT), which allows determination of both the form factor and the structure factor without assuming a model for the shape of the particles.[28] The analytical procedure yields the pair distance distribution function $p(r)$, which contains in its form information on the geometrical features (size and shape) of the scattering object. For the analysis of interactions near cloud points, the structure factor was modeled with the modified Ornstein−Zernike function:[29]

$$S(q) = 1 + \frac{\rho k_B T \chi_T}{1 + q^2 \xi_c^2} \quad (3)$$

where ρ is the particle number density, χ_T is the isothermal osmotic compressibility, and ξ_c is the correlation length of the concentration fluctuation. χ_T and ξ_c are adjustable parameters determined through the GIFT procedure.

Results

Phase Behavior of $C_i\beta G_1$/PEG in Ammonium Sulfate Solutions. The clouding behavior of $C_8\beta G_1$ and $C_9\beta G_1$ was studied in aqueous solutions with ammonium sulfate. For solutions of $C_9\beta G_1$ up to 10 wt % no macroscopic phase separation can be observed from 0 to 100 °C when the buffer contains less than 1.3 M ammonium sulfate (4 M ionic strength). In the case of $C_8\beta G_1$, this critical salt concentration is shifted to about 2 M (6 M ionic strength), which is in agreement with a previous study.[30] In solution with 0.5 M ammonium sulfate, both alkyl monoglucosides form a single homogeneous liquid phase up to 25 wt % surfactant and 100 °C. This salt concentration was therefore chosen to assess the effect of PEG on the clouding behavior of both alkyl monoglucosides over an extended range of concentration and temperature.

The phase behavior of pure PEG solutions with 0.5 M ammonium sulfate was also determined. These solutions form a single isotropic phase at low temperature and exhibit a liquid−liquid phase transition with increasing temperature. The cloud temperature of the PEG solutions decreases with increasing polymer molecular weight or concentration. For PEG of molecular weight 3350 g·mol^{-1} or larger, the liquid−liquid phase transition in the 0.5 M ammonium sulfate buffer occurs at temperatures below 100 °C.

Figure 1 shows the phase behavior of mixtures of $C_8\beta G_1$ and $C_9\beta G_1$ with PEG 3350. The addition of the surfactant lowers the upper phase boundary somewhat with respect to that of the PEG/solvent system and induces a new miscibility gap at low temperatures, where mixtures phase separate on cooling. The extent of the lower two-phase region depends strongly on the length of the surfactant carbon chain, and thus on its solubility, while replacement of $C_8\beta G_1$ by $C_9\beta G_1$ has only a small effect on the upper phase boundary. Varying the relative amount of polymer and surfactant in the mixture (δ) also affects the lower miscibility region more strongly than the upper one.

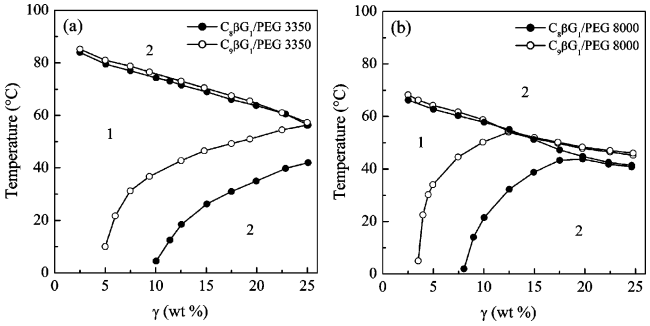

Figure 1. Pseudo-binary-phase diagrams of $C_i\beta G_1$/PEG 3350 mixtures (a) and $C_i\beta G_1$/PEG 8000 mixtures (b) with $\delta = 80\%$ showing the effect of surfactant tail length. Mixtures are dissolved in a buffered solution (25 mM potassium phosphate, pH 5.5) with 0.5 M ammonium sulfate. Cloud points are determined with an accuracy of ± 0.1 °C.

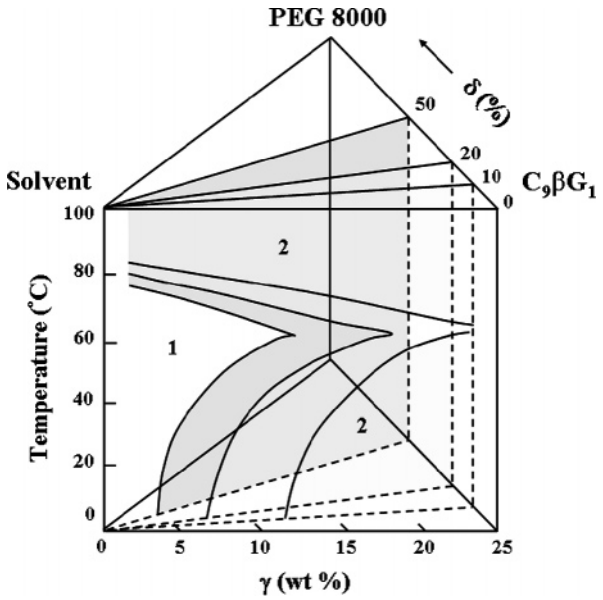

Figure 2. Glucoside-rich corner ($\delta \leq 50\%$) of the Gibbs phase prism showing the merging of the lower and upper two-phase regions with increasing δ for $C_9\beta G_1$/PEG 8000 mixtures in 0.5 M ammonium sulfate solution (25 mM potassium phosphate, pH 5.5).

The evolution of the two-phase regions as a function of δ in $C_9\beta G_1$/PEG 8000 mixtures is reported in Figure 2. With increasing amounts of polymer, the lower region extends to higher temperatures and lower values of γ, whereas the phase transition temperatures of the upper region decrease. At the end of the range, increasing δ causes the lower miscibility region to shrink until it disappears in solutions of pure PEG 8000 ($\delta = 100\%$) as shown in Figure 3. The maximum extension of the lower miscibility gap is reached for values of δ of about 60%. For values of δ above this value a different trend is observed, with the appearance of a narrow one-phase channel, approximately 1 °C wide, that separates the upper and lower miscibility gaps at high concentrations (γ) (Figure 3). The channel shifts to lower temperatures with increasing δ, but it is always above the phase transition temperature of the corresponding pure PEG solution. Mixtures falling within this channel appear macroscopically homogeneous, but they are opaque and display a weak birefringence when observed between crossed polarizers (inset in

(27) Glasoe, P. K.; Long, F. A. *J. Phys. Chem.* **1960**, *64*, 188−190.
(28) Brunner-Popela, J.; Glatter, O. *J. Appl. Crystallogr.* **1997**, *30*, 431−442.
(29) Glatter, O.; Fritz, G.; Lindner, H.; Brunner-Popela, J.; Mittelbach, R.; Strey, R.; Egelhaaf, S. U. *Langmuir* **2000**, *16*, 8692−8701.
(30) Lorber, B.; DeLucas, L. J.; Bishop, J. B. *J. Cryst. Growth* **1991**, *110*, 103−113.

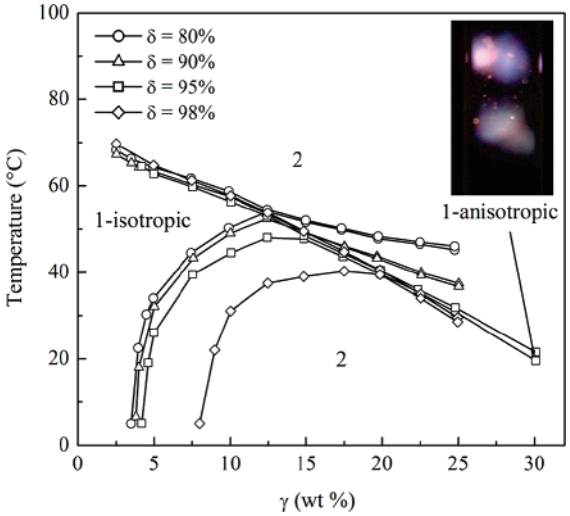

Figure 3. Projection of pseudo-binary phase diagrams of $C_9\beta G_1$/PEG 8000 mixtures with δ between 80% and 98% in buffer with 0.5 M ammonium sulfate. The photograph in the inset shows the mixture with $\delta = 95\%$ and $\gamma = 30$ wt % at 21 °C when held between crossed polarizers. Cloud points are determined with an accuracy of ± 0.1 °C.

Figure 3). The nature of this phase is difficult to assess because of the narrow range of temperature over which it occurs and the small density difference between the separating phases. However, the weak birefringence is consistent with the observation that ordered regions with long-range interactions form near phase boundaries,[31] and here this phenomenon may be enhanced due to the close proximity of two phase transitions.

Further insight into the one-phase channel was gathered by analyzing the volume and composition of the equilibrium phases of samples in the upper and lower miscibility gap with the same values of γ (Supporting Information, Table S1). In the lower miscibility region, a large top phase is generally in equilibrium with a considerably smaller and more viscous bottom phase, whereas in the upper region right above the one-phase channel the distribution of volumes is reversed. The concentration of the alkyl monoglucoside surfactant in each phase was determined using the anthrone method. Results of the colorimetric assay show that the surfactant partitions preferentially in the bottom phase for samples in the lower miscibility region, whereas it enriches the top phase in the upper two-phase region. Therefore, the narrow channel serves as a separation line between two miscibility regions where the surfactant-rich phases are inverted.

This unusual behavior was not observed at values of δ lower than 60%. For $\delta = 50\%$ and values of γ above 14 wt % the two regions merge, and mixtures separate into two isotropic liquid phases over all of the temperature range from 0 to 100 °C (Figure 2). In this miscibility region, however, the dynamics and morphology of the phase separation vary distinctly with temperature. A region of fast phase separation is observed at temperatures between 50 and 70 °C, with domains growing and coalescing on the time scale of seconds. Once the domains reach a few millimeters in size their density differences are large enough that they separate. A few minutes are generally sufficient for these mixtures to form two clear liquid phases separated by a sharp meniscus. Outside this region, phase separation occurs very slowly, and the system may need days to reach equilibrium.

The colorimetric method with anthrone was used to determine the tie lines of the lower miscibility regions in the ternary phase

(31) Koehler, R. D.; Schubert, K. V.; Strey, R.; Kaler, E. W. *J. Chem. Phys.* **1994**, *101*, 10843−10849.

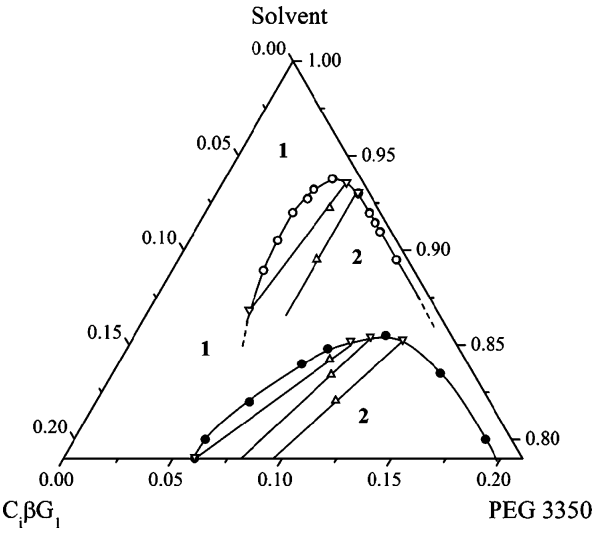

Figure 4. Ternary phase diagrams with tie lines for $C_8\beta G_1$/PEG 3350 (●) and $C_9\beta G_1$/PEG 3350 (○) mixtures in 0.5 M ammonium sulfate buffer (25 mM potassium phosphate, pH 5.5) at 25 °C. Concentrations are given in mass fractions.

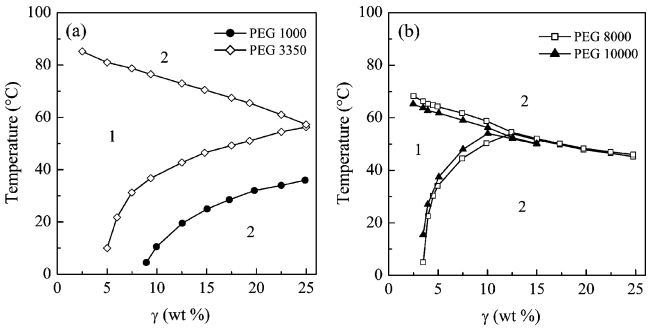

Figure 5. Pseudo-binary phase diagram ($\delta = 80\%$) of mixtures of $C_9\beta G_1$ and PEG with molecular weights 1000, 3350, 8000, and 10 000 in 0.5 M ammonium sulfate buffer. Cloud points are determined with an accuracy of ± 0.1 °C.

diagrams at 25 °C. Note that the full composition was not measured for each sample, but rather tie lines were drawn from points placed on the boundaries of the two-phase region after quantifying the amount of the alkyl glucoside component in each phase at equilibrium. Figure 4 shows the dilute portion of ternary phase diagrams of $C_8\beta G_1$ and $C_9\beta G_1$ with PEG 3350 at 25 °C with concentrations of polymer and surfactant up to 20 wt %. The initial compositions of the mixtures used to determine the tie lines of the miscibility region are also shown. Phase boundaries for these mixtures show similar patterns to those in mixtures that undergo a segregative type separation. However, the tie lines are not horizontal, which indicates an uneven distribution of the components in the two phases at equilibrium. In both miscibility gaps at 25 °C the alkyl monoglucosides partition strongly into the bottom phase, while the polymer enriches the top phase to a smaller extent.

The effect of PEG molecular weight on the phase transition boundaries of $C_9\beta G_1$/PEG mixtures ($\delta = 80\%$) is shown in Figure 5. In combinations with PEG 1000 only the lower miscibility gap is observed, whereas for PEG 3350 and above the upper miscibility gap drops into the region below 100 °C. In $C_9\beta G_1$/PEG 8000 mixtures and for values of γ larger than 10 wt %, the two miscibility regions are separated by a narrow one-phase channel, which closes at higher molecular weights of PEG. For mixtures of $C_9\beta G_1$/PEG 400 and $C_8\beta G_1$/PEG 400 in the 0.5 M ammonium sulfate buffer no phase transitions are evident up to $\gamma = 25$ wt %.

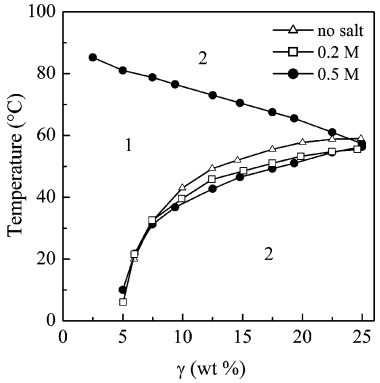

Figure 6. Pseudo-binary phase diagrams of $C_9\beta G_1$/PEG 3350 mixtures ($\delta = 80\%$) for different concentrations of ammonium sulfate in phosphate buffer solution: no salt, 0.2 M, and 0.5 M. Cloud points are determined with an accuracy of ± 0.1 °C.

Table 1. Micellization Properties from ITC Experiments for $C_8\beta G_1$ and $C_9\beta G_1$ in Solution with PEG 3350 and 0.5 M Ammonium Sulfate at 25 °C

	$C_8\beta\mathbf{G}_1$		$C_9\beta\mathbf{G}_1$	
PEG 3350 (wt %)	CMC (mM)	$\Delta G^o_{mic_{pol}} - \Delta G^o_{mic}$ (kJ/mol)	CMC (mM)	$\Delta G^o_{mic_{pol}} - \Delta G^o_{mic}$ (kJ/mol)
0	14.6		3.7	
2	15.5	0.20	3.9	0.18
4	16.5	0.40	4.3	0.47
6	17.1	0.54	4.8	0.79
8	17.9	0.71	5.1	1.00
10	18.5	0.84	5.5	1.23

Figure 6 shows the effect of ammonium sulfate concentration on the pseudo-binary phase diagram of $C_9\beta G_1$/PEG 3350 mixtures with $\delta = 80\%$. The upper two-phase region occurs at $T < 100$ °C only for the buffer with 0.5 M ammonium sulfate, whereas mixtures in pure water and buffer with 0.2 M salt display only the lower miscibility gap. This trend follows the observation that solutions of PEG 3350 in water and 0.2 M buffer for concentrations up to 25 wt % form one homogeneous phase from 0 to 100 °C. Varying the concentration of ammonium sulfate has a negligible effect on the lower two-phase region when γ is below 10 wt %, whereas for $\gamma > 10$ wt % the cloud temperature decreases with increasing salt concentration.

Micellization of $C_i\beta G_1$ in PEG Solutions. Isothermal titration calorimetry was used to measure the enthalpy of mixing of $C_8\beta G_1$ and $C_9\beta G_1$ injected into solutions with fixed concentrations of PEG 3350. For both surfactants, the trend in the enthalpy curves as a function of surfactant concentration exhibits an inversion when the concentration of the polymer is increased, and the enthalpy of micellization becomes negative (Supporting Information, Figures S1 and S2). For $C_8\beta G_1$/PEG 3350 mixtures the crossover occurs at PEG concentrations of about 8 wt %, and it shifts to lower concentrations (~5 wt %) in mixtures with $C_9\beta G_1$.

The CMCs of the alkyl monoglucosides in solution with PEG 3350 were determined by differentiation of the ITC enthalpograms (Table 1) as described above. For both surfactants, addition of the polymer causes an increase in the CMC. In surfactant−polymer systems where complexation occurs, CMCs generally decrease with increasing polymer concentration.[32] The surfactant enthalpies of micellization (ΔH_{mic}) were determined from the baseline in the micellar and monomer region of the enthalpograms according to

$$\Delta H_{mic} = \Delta H_{micelle} - \Delta H_{monomer} \quad (4)$$

Standard free energies of micellization were calculated from[33]

$$\Delta G^o_{mic} = \mu^o_{mic} - \mu^o_w = RT \ln X_{CMC} \quad (5)$$

where μ^o_{mic} and μ^o_w are the standard chemical potentials of the surfactant monomer in the micelle and in the dilute solution, and X_{CMC} is the surfactant mole fraction at the CMC. The properties of micelle formation of $C_8\beta G_1$ and $C_9\beta G_1$ in solution with PEG 3350 and 0.5 M ammonium sulfate from ITC experiments at 25 °C are shown in Figure 7. The enthalpy contribution to the standard free energies is very small as compared to the entropy term, and changes sign with increasing PEG concentration at about 8.5% and 5% in mixtures with $C_8\beta G_1$ and $C_9\beta G_1$, respectively. The entropy term is always positive and decreases with increasing concentration of the polymer.

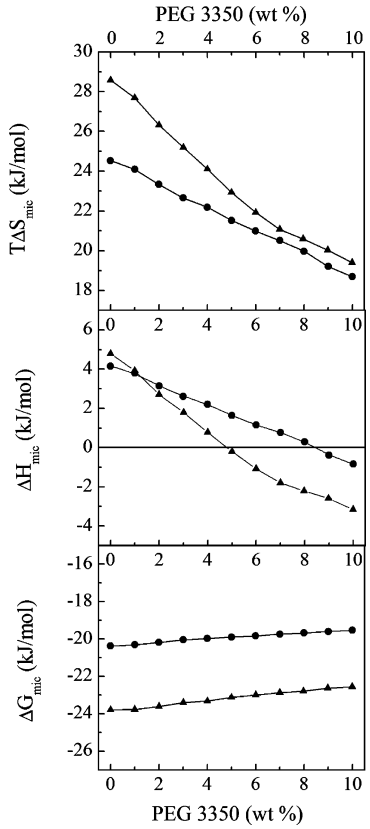

Figure 7. Micellization properties of $C_8\beta G_1$ (●) and $C_9\beta G_1$ (▲) as a function of PEG 3350 concentration in solutions with 0.5 M ammonium sulfate from ITC experiments at 25 °C.

A quantitative assessment of the polymer−micelle interaction is available by calculating the difference between the standard free energy changes of micellization in the presence and absence of polymer as given by[34]

$$\Delta G^o_{mic_{pol}} - \Delta G^o_{mic} = RT \ln\left(\frac{X_{CMC_{pol}}}{X_{CMC}}\right) \quad (6)$$

where $X_{CMC_{pol}}$ is the CMC in the presence of polymer in units of mole fraction. From this equation, a positive difference in the

(32) Brackman, J. C.; Engberts, J. B. F. N. In *Structure and Flow in Surfactant Solutions*; Herb, C. A., Prud'homme, R. K., Eds.; American Chemical Society: Washington, DC, 1994; Vol. 578, pp 337−349.

(33) Tanford, C. *The Hydrophobic Effect: Formation of Micelles and Biological Membranes*, 2nd ed.; Wiley & Sons: New York, 1980.

(34) Tokiwa, F.; Tsujii, K. *Bull. Chem. Soc. Jpn.* **1973**, *46*, 2684−2686.

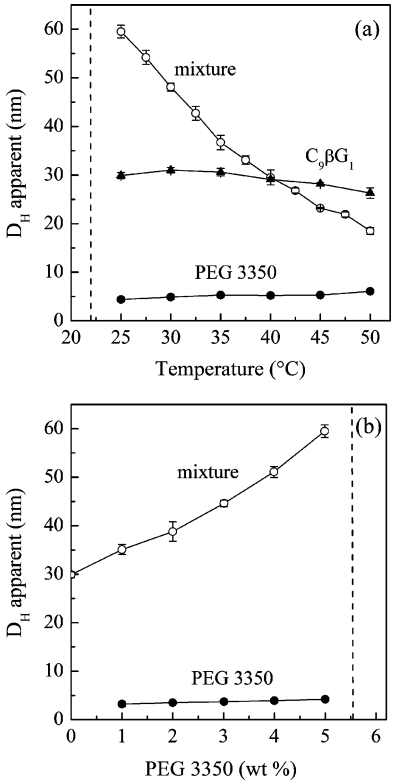

Figure 8. Mean apparent hydrodynamic diameter at 25 °C from DLS experiments of $C_9\beta G_1$/PEG 3350 mixtures as a function of temperature (a) (at fixed surfactant and polymer concentrations of 1 wt % and 5 wt %, respectively) and as a function of polymer composition (b). Mixtures (○) are shown along with the surfactant-free solutions of PEG 3350 (●) and of $C_9\beta G_1$ (▲). All buffers contain 0.5 M ammonium sulfate. The dashed lines indicate the point of phase separation of the mixture.

Gibbs free energies indicates that the interaction between polymer and micelle is not energetically favorable. For all combinations of the $C_i\beta G_1$ and PEG 3350 used here, $\Delta G^o_{mic_{ppl}}$ is always larger than the corresponding standard free energy in the absence of PEG, and their difference becomes larger with increasing polymer concentration (Table 1). In mixtures of $C_9\beta G_1$ and PEG 3350 the difference $\Delta G^o_{mic_{pol}} - \Delta G^o_{mic}$ is larger than in mixtures of $C_8\beta G_1$ at the same polymer concentration. These results confirm quantitatively the less favorable interactions of PEG with $C_9\beta G_1$ with respect to $C_8\beta G_1$, which is anticipated from the phase behavior patterns, since phase segregation occurs in the former mixtures at lower concentrations than in the latter.

Light Scattering from $C_i\beta G_1$/PEG Mixtures. Dynamic light scattering was used to measure the apparent hydrodynamic diameters of aggregates in homogeneous solutions as conditions approach a transition point on the liquid−liquid phase boundary. Both paths at constant temperature and varying polymer concentration or constant composition and varying temperature were explored. In both cases, the concentration of the alkyl monoglucosides ($C_8\beta G_1$ and $C_9\beta G_1$) was kept fixed at 1 wt %, and samples were prepared in the buffer with 0.5 M ammonium sulfate.

The apparent hydrodynamic diameter for solutions of $C_9\beta G_1$ as a function of PEG 3350 and temperature (with the PEG 3350 concentration fixed at 5 wt %) are shown in Figure 8, panels a and b, respectively. When solution conditions approach a phase transition point in the lower miscibility region a drastic increase of the micellar apparent hydrodynamic size (D_H) is observed. Similarly, the measured apparent D_H for solutions of $C_8\beta G_1$ (1 wt %) becomes larger as the PEG 3350 concentration increases

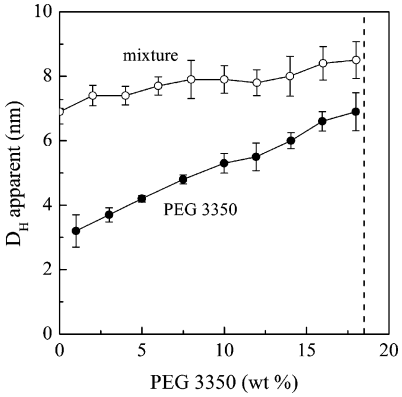

Figure 9. Mean apparent hydrodynamic diameter from DLS experiments for $C_8\beta G_1$/PEG 3350 mixtures (○) and surfactant-free solutions of PEG 3350 (●). Experiments performed at 25 °C in phosphate buffer with 0.5 M ammonium sulfate and constant surfactant concentration (1 wt %). The dashed line indicates the point of phase separation of the mixture.

up to 18 wt % (Figure 9). In these mixtures, however, the increase of D_H is much less dramatic than it is for $C_9\beta G_1$/PEG 3350. The increase of the apparent size measured by dynamic light scattering can be ascribed to either or both micellar growth and an increase in attractive interactions, and these experiments alone are not sufficient to distinguish between the two mechanisms.

Small-Angle Neutron Scattering from $C_i\beta G_1$/PEG Mixtures. The microstructure and interactions in mixtures of $C_i\beta G_1$ and PEG 3350 were characterized by small-angle neutron scattering experiments at constant temperature along paths with fixed δ and varying γ. The values of γ for the $C_8\beta G_1$/PEG 3350 and $C_9\beta G_1$/PEG 3350 mixtures examined were chosen to be at the same distance in relative composition from the phase boundary, so that they have comparable values of the reduced concentration, γ_{red}, defined as

$$\gamma_{red} = \left| \frac{\gamma - \gamma_{cloud}}{\gamma_{cloud}} \right| \qquad (7)$$

Here γ_{cloud} is the total concentration of surfactant and polymer at which liquid−liquid phase separation occurs. Mixtures in the D_2O buffer used for SANS exhibit transition points at values of γ that are approximately 2 wt % lower than in the corresponding H_2O solutions. Strong isotope effects have been reported for alkyl glucoside surfactants, as a consequence of the change in strength of the hydrogen bonds in the highly hydrophilic head group shell.[35] In general, these effects have been reported to be stronger in solutions at high ionic strength.[36] Here, the CMCs of $C_8\beta G_1$ and $C_9\beta G_1$ were measured by ITC in both aqueous and deuterated buffers (25 mM potassium phosphate pH/pD 5.5) and showed no difference in both solutions without ammonium sulfate. In buffers with 0.5 M ammonium sulfate the CMC in the deuterated buffer is 0.5 mM lower than that in the aqueous buffer.

Figure 10 shows the scattering profiles from mixtures of glucosides and PEG 3350 with constant $\delta = 80\%$ and varying γ. Measurements were taken at 25 °C, and the scattering from the background salt solution (0.5 M ammonium sulfate) was subtracted. For both systems an increase at low values of the scattering vector q is observed on approach to the phase boundary, specifically on increasing the total concentration of glucoside and PEG up to the value of γ_{cloud}.

(35) Whiddon, C.; Soderman, E. *Langmuir* **2001**, *17*, 1803−1806.
(36) Chang, N. J.; Kaler, E. W. *J. Phys. Chem.* **1985**, *89*, 2996−3000.

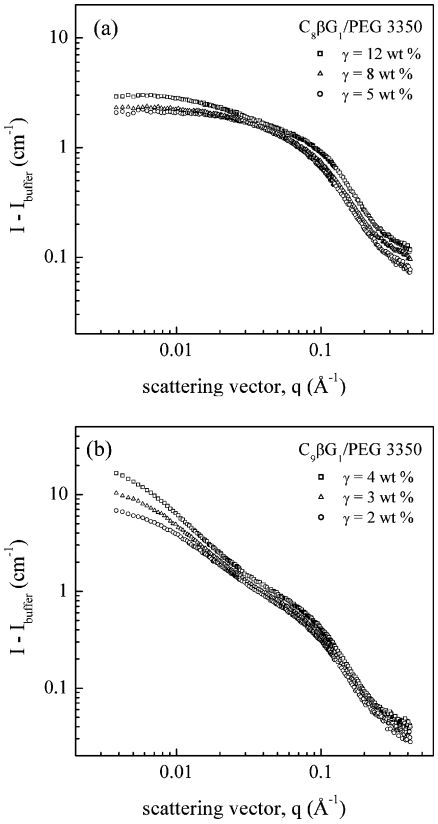

Figure 10. Scattering data for $C_8\beta G_1$/PEG 3350 (a) and $C_9\beta G_1$/PEG 3350 (b) mixtures with $\delta = 80\%$ and varying γ. Solvent is 0.5 M ammonium sulfate buffer (pH 5.5 with 0.025 M potassium phosphate) and $T = 25$ °C.

The pair distance distribution functions were obtained using the GIFT method and are reported in Figure 11. For $C_8\beta G_1$/PEG 3350 mixtures, $p(r)$ remains substantially the same for different values of γ, and in particular the maximum length is not affected significantly for γ from 5 to 12 wt %. Similar results were obtained for micelles of $C_9\beta G_1$ on addition of PEG 3350, for surfactant concentrations from 2 to 4 wt %. The effect of PEG on the strength (χ_T) and range (ξ_c) of micellar interactions is more significant. Figure 12 shows the values of $S(0)$ and ξ_c for both types of mixtures, with $S(0)$ defined as

$$S(0) = \rho k_B T \chi_T \tag{8}$$

$C_8\beta G_1$/PEG 3350 solutions are characterized by much smaller values of both $S(0)$ and ξ_c than are $C_9\beta G_1$/PEG 3350 mixtures, which indicates that interactions in the latter mixtures are stronger and longer-ranged than in the former.

In the case of $C_8\beta G_1$/PEG 3350 mixtures, with relatively small values of $S(0)$, a first-order expansion of the osmotic pressure can be used to evaluate the osmotic second virial coefficient B_{22}, using the expressions

$$\frac{1}{k_B T}\left(\frac{\partial \Pi}{\partial \rho}\right)_T = 1 + 2B_{22}\rho + \ldots \tag{9}$$

$$S(0) \cong \frac{1}{1 + 2B_{22}\rho} \tag{10}$$

The number density of the micelles (ρ) was calculated from the volume fraction of the surfactant in the micellar state and the volume of the micelles, which were assumed to be prolate ellipsoids with dimensions as determined from the GIFT analysis.

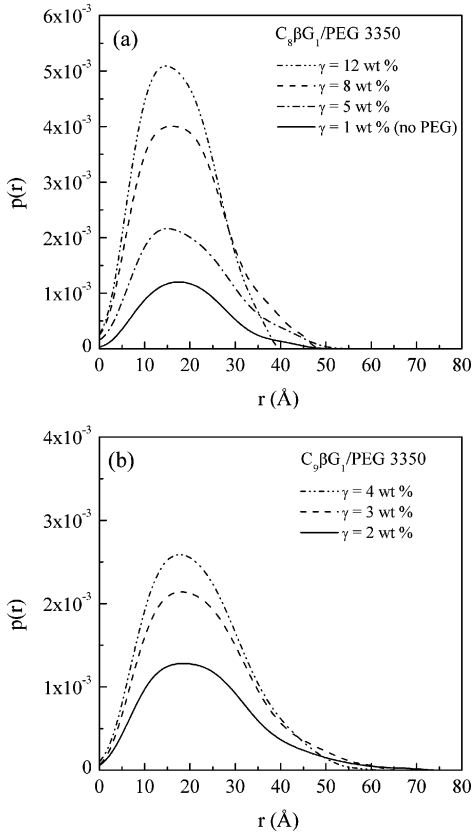

Figure 11. Pair distance distribution function from GIFT analysis for $C_8\beta G_1$/PEG 3350 (a) and $C_9\beta G_1$/PEG 3350 (b) mixtures with $\delta = 80\%$ and varying γ ($T = 25$ °C).

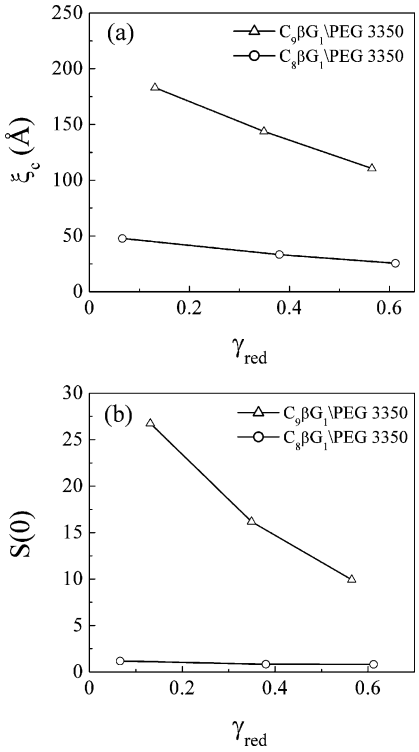

Figure 12. Correlation length (a) and structure factor at $q = 0$ (b) from GIFT analysis for mixtures of PEG 3350 with $C_8\beta G_1$ and $C_9\beta G_1$ with $\delta = 80\%$ and varying γ ($T = 25$ °C).

Figure 13a shows the value of B_{22} normalized by the hard sphere value B_{22}^{HS} for solutions of $C_8\beta G_1$ in PEG 3350. The values of B_{22}^{HS} for the ellipsoidal micelles were calculated using the method

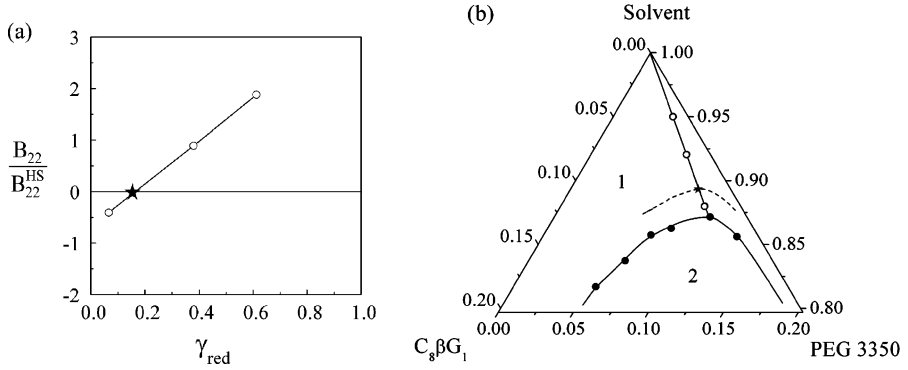

Figure 13. Reduced B_{22} as a function of reduced surfactant concentration (left panel) and mapped onto the ternary diagram (right panel). B_{22} values will be slightly negative in the region between the dashed line and the phase boundary (in the so-called crystallization slot). Data is for $C_8\beta G_1$/PEG 3350 mixtures with $\delta = 80\%$ in deuterated buffer (25 mM potassium phosphate, pD 5.5) with 0.5 M ammonium sulfate at 25 °C.

of Harding et al.[37] Results show that in this system the nature of micellar interactions changes from repulsive to attractive with decreasing γ_{red} and as the cloud point is approached. For mixtures with $\delta = 80\%$, this transition occurs when γ_{red} reaches the critical value of 0.16, which corresponds to $\gamma = 10.7$ wt %. This point can be mapped on the ternary phase diagram to shape the boundary of a region characterized by negative values of B_{22} (Figure 13b).

Discussion

By investigating the phase behavior of mixtures of the alkyl monoglucosides $C_8\beta G_1$ and $C_9\beta G_1$ and PEG as a function of the relative ratio of the polymer and surfactant (δ), total concentration (γ), and molecular weight, we have found interesting patterns of phase transitions at temperatures suitable for biological separation processes. Specifically, for PEG of molecular weights 3350 and 8000 and in solutions with 0.5 M ammonium sulfate, both lower and upper miscibility gaps can be observed. These regions can be made to merge by increasing either the amount of polymer in the mixture or the polymer molecular weight. The collision of the upper and lower miscibility gaps has been observed for mixtures of C_8E_4 and PEG with increases in polymer molecular weight[5] and follows the same trend as in solutions of polystyrene and organic solvents.[38] Here, the presence of a narrow channel between the miscibility regions can be observed for mixtures of $C_9\beta G_1$ and PEG 8000 with high polymer mass fractions (δ). This small one-phase region exists because the surfactant partitions preferentially into the top phase in the upper miscibility gap and into the bottom phase in the lower region, so the tie lines of the lower and upper miscibility regions have dramatically different slopes. This one-phase region bordered by two phase transitions only a few degrees away introduces new windows of interactions that could be used to direct the ordering of colloids and proteins.

The upper miscibility gap in $C_i\beta G_1$/PEG mixtures exhibits minimal changes when the alkyl chain of the amphiphile is varied and follows the same trend as the pure polymer solutions. This evidence is an indication that phase separation at high temperatures is driven mainly by changes of the polymer structure. On the contrary, lower miscibility gaps in both mixtures display a sharp difference as a consequence of surfactant substitution or changes in the relative amounts of surfactant and polymer (δ). In both cases, the choice of the surfactant is crucial to define optimal regions for membrane protein crystallization, which is typically carried out around room temperature (20−25 °C) and at low surfactant concentration (∼1 wt %). Salt concentration is an additional variable commonly exploited to tune solution conditions for optimal crystallization. The negligible difference observed in the phase transition boundaries at low values of γ (Figure 6) is an indication that the intermicellar interactions are not affected strongly by varying the concentration of ammonium sulfate.

Isothermal titration calorimetry is a sensitive thermodynamic technique useful for studying interactions between molecules in solution and has been applied to several polymer/surfactant systems.[39] When association of the polymer and surfactant occurs, the heat evolved from the binding event will give an additional peak before the micellization point is visible on the ITC enthalpy diagrams. Specifically for PEG, complexation has been shown to occur in combination with ionic surfactants such as SDS[40,41] or cesium perfluorooctanoate.[42] For the class of nonionic alkyl polyglucosides, Brackman et al. have found that complexation occurs between *n*-octyl thioglucoside and hydrophobic polymers such as polypropylene oxide (PPO) but not with the more hydrophilic PEG.[43]

Here, ITC was used to characterize the interactions between PEG and the alkyl monoglucosides $C_8\beta G_1$ and $C_9\beta G_1$, and to gain insight into the mechanism of phase separation of these mixtures. Micelle formation is an entropy-driven cooperative process wherein the hydrophobic effect, which favors association, is balanced by the repulsion between head groups. For nonionic surfactants this repulsion is principally a steric repulsion because the head group interactions are short ranged. As the polymer concentration increases, surfactant head groups experience an increase in steric hindrance, which is reflected in the increase of the CMC and a reduction of the value of the standard free energy of micellization. At the same time, the decrease in the entropy of micellization of $C_i\beta G_1$ in solutions with PEG can be accounted for by the change in hydration of the surfactant head group caused by competition for water with the highly hydrophilic polymer. Alkyl-β-monoglucosides have strongly hydrated head groups and PEG solutions become a less good solvent for the surfactant with increasing polymer concentration. Similar trends in the enthalpy change of micellization with added polymer are observed for other nonionic surfactants, including octyl glucoside, on increasing the temperature, and have been related to hydration

(37) Harding, S. E.; Horton, J. C.; Jones, S.; Thornton, J. M.; Winzor, D. J. *Biophys. J.* **1999**, *76*, 2432−2438.
(38) Siow, K. S.; Patterson, D.; Delmas, G. *Macromolecules* **1972**, *5*, 29−34.
(39) Bloor, D. M.; Holzwarth, J. F.; Wynjones, E. *Langmuir* **1995**, *11*, 2312−2313.
(40) Wang, G.; Olofsson, G. *J. Phys. Chem. B* **1998**, *102*, 9276−9283.
(41) Dai, S.; Tam, K. C. *J. Phys. Chem. B* **2001**, *105*, 10759−10763.
(42) Gianni, P.; Barghini, A.; Bernazzani, L.; Mollica, V.; Pizzolla, P. *J. Phys. Chem. B* **2006**, *110*, 9112−9121.
(43) Brackman, J. C.; van Os, N. M.; Engberts, J. B. F. N. *Langmuir* **1988**, *4*, 1266−1269.

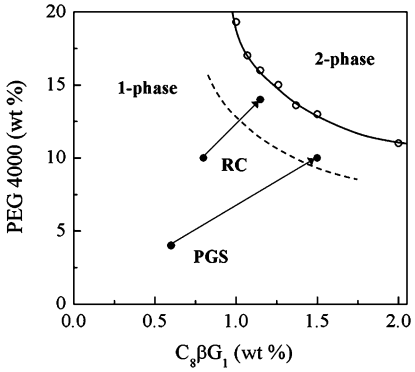

Figure 14. Crystallization conditions of the reaction center of *R. sphaeroides* (RC) and of prostaglandin H synthase (PGS) near the liquid−liquid phase boundary of $C_8\beta G_1$/PEG 4000 mixtures with 0.4 M NaCl (adapted from Garavito and Picot[46]). The dashed line denotes the region where attractive interactions occur as determined in our SANS studies from $C_8\beta G_1$/PEG 3350 mixtures.

changes of the head groups at elevated temperatures.[44] In addition, ITC measurements reveal the development of a small shoulder around the CMC of $C_9\beta G_1$ in the presence of 10 wt % PEG 3350 (Supporting Information, Figure S2). Experiments using ITC to measure solutions of alkyl trimethylammonium surfactants show that this feature, specifically an increase of the enthalpy of dilution before the CMC, is related to a nonideal component of the solution thermodynamics.[45] In mixtures with PEG this trend is more evident with $C_9\beta G_1$ than with the shorter $C_8\beta G_1$, and it is consistent with the Gibbs free energy calculation of polymer-micelle interactions (Table 1) and with the SANS analysis of the effect of PEG on the range and strength of intermicellar interactions.

Light scattering shows a drastic increase of the apparent hydrodynamic diameter in $C_9\beta G_1$/PEG 3350 mixtures as solution conditions approach the liquid−liquid phase boundary on paths at constant temperature or composition. On the other hand, in $C_8\beta G_1$/PEG 3350 mixtures the increase of the apparent diameter is much smaller over the same range of distance from the cloud point. Such increases can be attributed either to an increase of the attractive interactions or to micellar growth, and light scattering alone is not sufficient to distinguish between the two mechanisms.

In small-angle neutron scattering, the GIFT model-independent analysis can separate information from micellar size and interactions and further characterize the strength of the interactions in terms of the osmotic second virial coefficient (B_{22}). In mixtures of $C_8\beta G_1$ and PEG 3350, interactions change from repulsive ($B_{22} > 0$) to attractive ($B_{22} < 0$) at 2.1 wt % from the cloud point ($\gamma_{cloud} = 12.8$ wt %), that is when γ_{red} is less than 0.16. Furthermore, for these mixtures interactions in this window are weak, as indicated by the reduced B_{22} values falling in the range from 0 to −1. This SANS analysis can be successfully related to actual crystallization conditions of membrane proteins available in the literature. Garavito and Picot report that the reaction center of *R. sphaeroides* (RC) and prostaglandin H synthase (PGS) form crystals in proximity of the liquid−liquid phase transition of $C_8\beta G_1$/PEG 4000 mixtures (Figure 14).[46] Crystallization conditions for RC and PGS are achieved at values of γ_{red} equal to 0.07 and 0.13, respectively, which are within the crystallization window identified by our SANS analysis. The crystallization experiments were carried out by vapor diffusion, so the relative amount of polymer and surfactant (δ) is constant, although their concentrations change during the crystallization process. The values of δ are 92% and 87% for crystallization of RC and PGS, respectively, which is comparable to the mixtures measured by SANS here. These results support the observation that crystallization conditions correlate with weak attractive interactions between the surfactant aggregates and that these interactions occur in proximity of the phase transition of the surfactant solution. SANS can be used to quantify the strength and range of such interactions, which can be very different even between systems where the surfactant alkyl chain differs by just one methylene group.

(44) Paula, S.; Sus, W.; Tuchtenhagen, J.; Blume, A. *J. Phys. Chem.* **1995**, *99*, 11742−11751.

(45) Bijma, K.; Engberts, J.; Blandamer, M. J.; Cullis, P. M.; Last, P. M.; Irlam, K. D.; Soldi, L. G. *J. Chem. Soc. Faraday Trans.* **1997**, *93*, 1579−1584.

(46) Garavito, R. M.; Picot, D. *Methods* **1990**, *1*, 57−69.

Conclusions

Mixtures of medium chain alkyl-β-monoglucosides and PEG are characterized by the simultaneous presence of an upper and lower miscibility gap in solutions with 0.5 M ammonium sulfate, when the polymer molecular weight is 3350 or larger. In combinations of PEG and octyl-β-glucoside the lower two-phase body is shifted to higher concentrations than is the case for nonyl-β-glucoside. For PEG 8000 at high values of δ and γ, a narrow one-phase channel where solutions are weakly birefringent separates two miscibility regions where the partitioning of the alkyl glucoside surfactant in the phases at equilibrium is strongly inverted.

Microcalorimetry measurements show that there is a stronger incompatibility in mixtures of PEG and $C_9\beta G_1$ than in combinations of the polymer with the shorter $C_8\beta G_1$. This results in a segregative phase separation that occurs at lower polymer concentrations and with larger miscibility gaps. Analysis of mixtures near the cloud point by SANS indicates that the role of PEG is to drastically change the strength and range of intermicellar interactions. PEG has minimal impact on the geometry of the micelles, and hence on related protein−surfactant complexes, so it is no surprise that PEG finds wide use in protein crystallization schemes. In the case of $C_8\beta G_1$/PEG 3350 combinations, the measured strength of the intermicellar interactions (the osmotic second virial coefficient B_{22}) can be related to successful crystallization conditions near the liquid−liquid phase transitions that are available in the literature.

Acknowledgment. We acknowledge the support of the National Institute of Standards and Technology, U.S. Department of Commerce, in providing the neutron research facilities used in this work, which were supported in part by the National Science Foundation under Agreement DMR-0454672. We thank S. Kline at NIST for technical assistance during data acquisition and G. Fritz at the University of Graz for the software used in the SANS analysis. The Center of Biomedical Research Excellence (COBRE) in Structural and Functional Genomics at the University of Delaware supported by the National Center for Research Resources at the NIH (Grant P20 RR015588) is acknowledged for use of the microcalorimeter. Funding for this work comes from the NASA Microgravity Research Program through Grant NAG8-1830.

Supporting Information Available: Composition of the equilibrium phases of $C_i\beta G_1$/PEG 3350 samples in the lower miscibility gap, enthalpy of mixing measured by ITC, analysis of SANS data with the GIFT method. This material is available free of charge via the Internet at http://pubs.acs.org.

LA063427D